Chemical Science

Non-equilibrium dynamic control of gold nanoparticle and hyper-branched nanogold assemblies†

Victor Sans,[a] Stefan Glatzel,[a] Fraser J. Douglas,[b] Donald A. Maclaren,[b] Alexei Lapkin[c] and Leroy Cronin*[a]

A flow system capable of dynamically controlling the synthesis of inorganic nanomaterials in real time switching between different conditions is presented whereby the combination of reactor engineering, ligand design and the employment of two in-line analytical techniques enables the synthesis and rapid characterisation of gold nanoparticles. Furthermore, it has been possible to discover a new type of hyper-branched nanogold-based material directly based on the optical feedback from UV-Vis, without stopping the process and the nanoparticles have been characterised using TEM.

The use of continuous-flow methods for the synthesis of inorganic materials, such as quantum dots, metal oxides and metallic nanoparticles holds great promise to develop new ways of manufacturing nanomaterials.[1] Despite the inherent processing advantages that flow chemistry offers due to an enhanced control over reaction conditions, and the facilitated scale-up, important challenges still preclude the widespread application of these technologies. The combination of microwave dielectric heating and flow chemistry has been successfully employed in organic chemistry,[2,3] but limited reports are available in the synthesis of inorganic nanostructured materials.[4,5] In addition, the precipitation of products in the reactor represents a major problem.[6] Recently, the synthesis of gold nanoparticles in microreactors using a precursor solution and a stabilizing agent has been reported,[6] but fouling of metal on the reactor walls, which could lead to reactor blockages, was observed. However, although the fouling issue can be partly overcome,[7] another major issue is the difficulty to characterise the products in real-time.[8]

Herein, we present an automated flow-system with real-time 'on the fly' dynamic control of the synthesis of gold nanoparticles (Au NPs). This is achieved by the combination of continuous-flow chemistr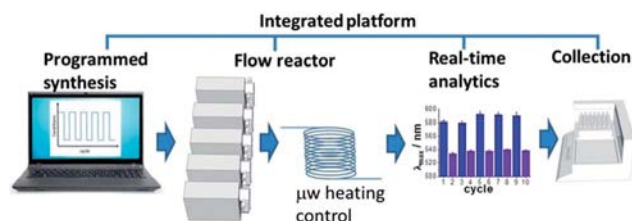y, microwave dielectric heating, and two in-line analytical techniques allowing instantaneous feedback: UV-Vis to measure the AuNP plasmon and dynamic light scattering (DLS) to determine the particle size distribution. Not only does this set-up allow the rapid optimisation of the reaction conditions, but also the dynamic control of the self-assembly processes involved in the synthesis of the nanoparticles. This allowed us to switch between different particle sizes/properties, with control of aggregation. For example this approached allowed us to discover a unique hyper-branched gold nanomaterial with a morphology that has never before been seen for gold, illustrating the potential of this approach.

The first reactor set-up consists of a set of PC controlled pumps (Tricontinent C3000) that feed reagents into a 4-way manifold made of polytetrafluoroethylene employed as mixer. The mixing occurred outside the heating chamber at room temperature and in a laminar regime. A U-tube fluorinated ethylene propylene FEP based tubing (1/8 inch OD, 1.58 mm ID) was employed as a reactor heated by a CEM Discovery microwave equipped with a flow-cell. The reactor was submerged in a glass-reinforced vessel filled with 10 mL of ethylene glycol (EG).

[a]*WestCHEM, School of Chemistry, University of Glasgow, Glasgow, G12 8QQ, UK. E-mail: Lee.Cronin@glasgow.ac.uk; Fax: +44 (0)141 330 4888; Tel: +44 (0)141 330 6650*

[b]*SUPA, School of Physics and Astronomy, University of Glasgow, Glasgow G12 8QQ, UK*

[c]*Department of Chemical Engineering and Biotechnology, University of Cambridge, Cambridge, CB2 3RA, UK*

† Electronic supplementary information (ESI) available: A detailed description of the reaction-set-up, results corresponding to UV-Vis under different experimental conditions, TEM images corresponding to the formation of aggregates and particle size distributions of the nanoparticles synthesized under flow. See DOI: 10.1039/c3sc53223b

Scheme 1 A schematic representation of the integrated platform for continuous-flow synthesis and in-line characterization of Au nanoparticles. The integration of hardware, software, reaction engineering, and real-time analytics offers the possibility of dynamically switching the properties of the synthesised nanostructured materials.

The microwave heats both the EG and the tube, generating a combined thermal/dielectric heating mode. After the reaction, an Avantes AvaSpec2048 spectrometer equipped with a flow cell collected the UV-Vis spectra and a NanoZS Malvern was employed to determine the particle size distribution. Finally, the nanoparticles were collected with a Gilson FC204 automated fraction collector. All the hardware was controlled and synchronised employing in-house developed LabView® software modules. For further details about the experimental set-up see ESI† (Scheme 1).

Initially, a solution of $HAuCl_4$ (0.2 mM in ethylene glycol) was mixed with citrate (4 mM in H_2O) at 0.5 mL min^{-1} and heated to 90 °C using a microwave. Under these conditions, the formation of nanoparticles was confirmed by UV-Vis. Spectra were continuously collected every 2 minutes and the baseline was automatically corrected and λ_{max} was calculated. An average maximum of 554 nm was initially observed with a standard deviation σ of 3.6 nm. This is consistent with broad particle size distributions.[9] The pH of the product solution was found to be 7.1 and under these conditions the reaction is expected to follow a classical nucleation-growth mechanism[10] where two effects contribute to this behaviour. Not only do walls of the tube act to facilitate nucleation, thus creating different particle sizes within the cross-section of the tube, a parabolic flow pattern introduces variability in the particle size distribution under laminar flow conditions.[11] Interestingly, a blue shift was observed after 150 min (see ESI Fig. S4†). This was due to the coating of Au on the inner surfaces of the reactor[12] and the extent of this coating was confirmed at the end of the reaction. At this point, the inner surface is completely covered by a metallic layer, which has a double effect. On one hand it modifies the interfacial properties of the reactor walls, thus reducing nucleation, and on the other hand improves the heating and heat transfer, due to the concentration of the microwave active metallic layer.[13] In this way, a second cycle under the same experimental conditions, showed averaged values of λ_{max} of 537 nm with σ 3.1 nm. Therefore the surface of the tube was engineered to take advantage of this process where a continuous layer of Au was generated by mixing a solution of precursor salt with a high concentration (2 mM) and reducing agent (20 mM). After two hours of flowing a 1 : 1 mixture of these reagents at low flow rate (0.25 mL min^{-1}) at 90 °C, a continuous gold layer is formed. It is worth noting that the nature of the tubing influenced the quality of the layer formed. When FEP was employed, a regular deposition was visually observed. Nevertheless, polytetrafluoroethylene (PTFE) showed a more irregular and discontinuous layer and the nature of the tubing has been reported previously to influence the deposition of Au in the reactor walls.[7] To reduce variability we introduced a hydrophobic self-assembled monolayer (SAM) onto previously deposited Au-coated tube surface by flowing a solution of 1-dodecanethiol (2 mM in EtOH) through the reactor (see ESI Fig. S5†).[14]

After the coating process the system proved to be much more robust, producing small nanoparticles with a very high level of reproducibility over time. Indeed, the averaged value of λ_{max} observed under flow conditions showed a blue-shift to *ca.*

532 nm with a very stable absorbance value and the particle size of the nanoparticles was found to be 7–8 nm by DLS. This result is consistent with the particle size determined by TEM (ESI Fig. S6†). Under these flow conditions, the linear velocity inside the DLS cell is *ca.* 0.05 mm s^{-1} and thus shear forces are not expected to affect the measurements.[15] The nanoparticles were stable for more than a month, with no noticeable changes in the extinction spectra (see ESI Fig. S7†). Our system is thus able to produce nanoparticles of a size similar or smaller than previously reported flow systems.[6] In any case this set-up produces AuNPs with small particle size, high reproducibility, stability and eliminates the potential problems related to reactor blockages from fouling.

To demonstrate the ability to dynamically control the self-assembly of the AuNPs, the ionic strength of the reaction media was progressively increased to 90 mM and then decreased accordingly. One pump was employed to provide the gold precursor at a constant flow rate (0.25 mL min^{-1}). Separately, solutions of citrate in H_2O and in borate buffer (pH = 9.2) were mixed with the $HAuCl_4$ in different proportions, thus changing the concentration of salts in the reaction media, but keeping the amount of citrate employed constant. The pH was controlled at different buffer concentrations and no differences were observed. Each reaction cycle lasted 20 minutes. Citrate is known to stabilize nanoparticles by an electrostatic mechanism.[16] Thus, a change in the ionic strength will modify the thickness of the double layer,[17] and hence affect the growth and aggregation processes of the nanoparticles and Fig. 2 summarizes the results. When a 0.2 mM solution of Au and 4 mM of citrate were mixed at different borate concentrations, two Local Surface Plasmon Resonance (LSPR) modes appeared in the UV-Vis spectra, indicating the coexistence of small nanoparticles with larger aggregates (see ESI, Fig. S8 for an example†). A red shift of the LSPR was observed when the ionic strength of the reaction medium was observed (Fig. 1a). The process proved to be reversible when the concentration of salts was progressively reduced after reaching a maximum concentration of salts of 90 mM. In-line DLS confirmed the increase of the particle size of the observed nanoclusters and TEM images
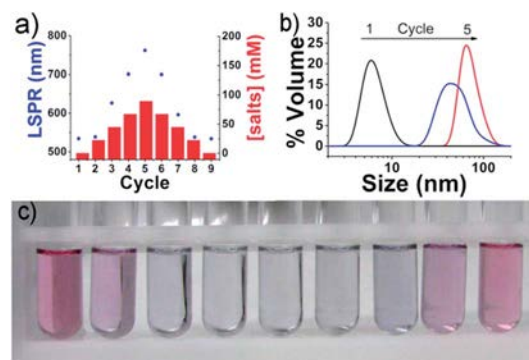

Fig. 1 Dynamic control of the dispersion/aggregation balance in the self-assembly of AuNPs. (a) LSPR values observed (blue dots) as a function of the buffer concentration (red bars). (b) Aggregation observed by on-line DLS as a result of the increase in the ionic strength. (c) Samples containing AuNPs collected in each cycle.
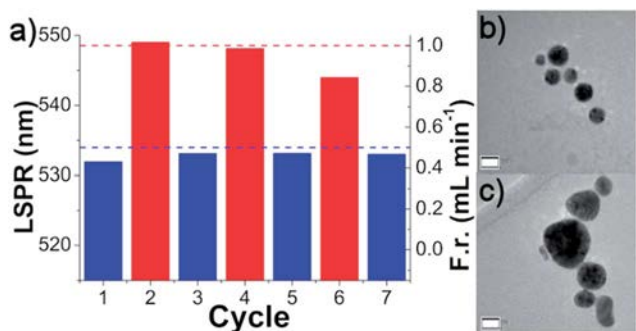
Fig. 2 Cycling experiment switching between equilibrium and non-equilibrium states at two different flow rates. (a) Plot of the LSPR as a function of the reaction cycle. Odd cycles correspond t_R 1.4 min and even to 0.7 min. (b) HRTEM image of the AuNP's obtained in cycle 1. Spherical shape predominates with an average size of 8.5 nm. White bar corresponds to a scale of 10 nm. (c) HRTEM image of the AuNP's obtained in cycle 2. Less spherical shape and wider particle size distribution. The white bar corresponds to a scale of 10 nm scale.

confirmed the presence of aggregated nanoparticles (ESI Fig. S9†).

A distinctive advantage of employing a fully automated flow set-up for the synthesis of nanostructured materials is that it opens the possibility of finely modifying the reaction conditions,[18,19] thus achieving a unique degree of control over their properties by varying not only the composition, but also system parameters such as the residence time of materials inside the reactor. Different concentrations of Au were employed to study the influence of the flow rate, keeping constant the Au : citrate ratio and it should be noted that the residence time of the nanoparticles in the reaction chamber plays a fundamental role in the properties of the nanoparticles. The extinction spectra collected 'on the fly' was compared with that measured two hours after finishing the flow experiments (ESI Fig. S10†).

Interestingly, at higher flow rates (lower residence times) the LSPR observed on the fly are higher than those observed after several hours. This result suggests that the nanoparticles have not yet reached the equilibrium after they leave the reactor. Moreover, at a residence time of 0.9 and 1.4 minutes the LSPR values are very similar in both measurements, indicating optimised conditions in which nanoparticles have reached an equilibrium and therefore are stable over time. Indeed, solutions with colours ranging from light pink to violet were obtained by decreasing the residence times from 2.8 to 0.5 minutes when a solution 0.2 mM of $HAuCl_4$ in ethylene glycol (EG) and a citrate : Au molar ratio of 20 were employed. At the lowest flow rate assayed, the resultant solution showed lower absorbance, higher LSPR and a broader shape compared to that obtained at slightly higher flow rates (ESI Fig. S11† shows a comparison of the UV-Vis spectra). This can be due to broader dispersion at low flow rates. Under optimal flow conditions (1.4 min residence time), pink solutions were reproducibly obtained with an LSPR of 532 nm. In-line DLS showed particle size distributions with averages ranging from 6 to 8 nm. At lower residence times under these experimental conditions, the ability of citrate to stabilise the nanoparticles seems to be less

effective. Indeed, further reductions in the residence time, produced stronger redshifts in the spectra corresponding to the in-line UV-Vis (ESI, Fig. S11†).

A cyclic experiment was designed to prove the ability to reversibly switch between two different states (equilibrium vs. non-equilibrium) by simply varying the residence time inside the reactor. The solutions employed were gold precursor ($HAuCl_4$ 2 mM in EG) and citrate (20 mM in H_2O). Initially, a 20 minutes cycle with a residence time of 1.4 minutes was carried out as a reference. Afterwards, the flow rate was increased to achieve a residence time of 0.7 minutes. This lasted 10 minutes and then the reference was again repeated. This was repeated to test the reproducibility of the results. The reference cycle showed consistently a LSPR of 533 nm. The higher flow rate produced in all cases nanoparticles with higher LSPR. A gradual blue shift was observed, from ca. 550 nm in cycle 2 to 545 nm in cycle 6. High Resolution Transmission Electronic Microscopy (HRTEM) images showed spherical particles with an average particle size of 7.5–8.5 nm (Fig. 2b). A decrease in the residence time to 0.7 min led to a redshift in the LSPR to higher wavelengths (550–545 nm). HRTEM images showed less spherical nanoparticles (Fig. 2c) with an average particle size of 11 nm and a broader particle size distribution.

To demonstrate the general validity of our approach to produce novel nanostructures and dynamically switch between different states we designed a new experimental rig, where the $HAuCl_4$ precursor can be premixed with two different ligands in a 4-way PEEK mixer manifold connected to a 0.5 mL tubular reactor (PTFE, 1/16″ OD, 1 mm ID). The gold-ligand mixture was subsequently mixed with a solution of ascorbic acid employing a 3-way PEEK mixer connected to a 1.5 mL tubular reactor (PTFE, 1/16″ OD, 1 mm ID), see Fig. 3a. The reactor was connected to the UV-Vis flow cell to allow real-time monitoring of the plasmon generated by the nanoparticles. Finally, the samples were collected in the FC204 for subsequent analysis.

Two ligands derived from the isonicotinamide were synthesised by reacting isonicotinoyl chloride with octyl and octadecylamine respectively to yield the corresponding amides N-octadecylisonicotinamide (L_1) and N-octylisonicotinamide (L_2), see Fig. 3d. Multiple supramolecular interactions, like hydrogen bonding between the amide and pyridine groups and van-der-Waals interaction of the hydrophobic chains were anticipated to play a role in controlling the faceting of the nanostructured materials. To the best of our knowledge these ligands have never been employed to stabilise nanoparticles. The dissolution of the ligands to the required concentration (2 mM) in water required sonication and heating the solutions with a heat gun and then keeping the solutions in a temperature controlled bath at 75 °C.

A cyclic experiment switching between the two ligands and keeping the rest of parameters constant was performed. Highly reproducible plasmons were observed in all the cycles, Fig. 3b. Each cycle ran for 5 minutes and spectra were collected the last two minutes at 5 second intervals. The error bars represent the standard deviation of the maximum LSPR detected in each cycle. In Fig. 3e, it can be observed that the spectra showed 3 well defined modes (538, 587 and 708 nm). Depending on the
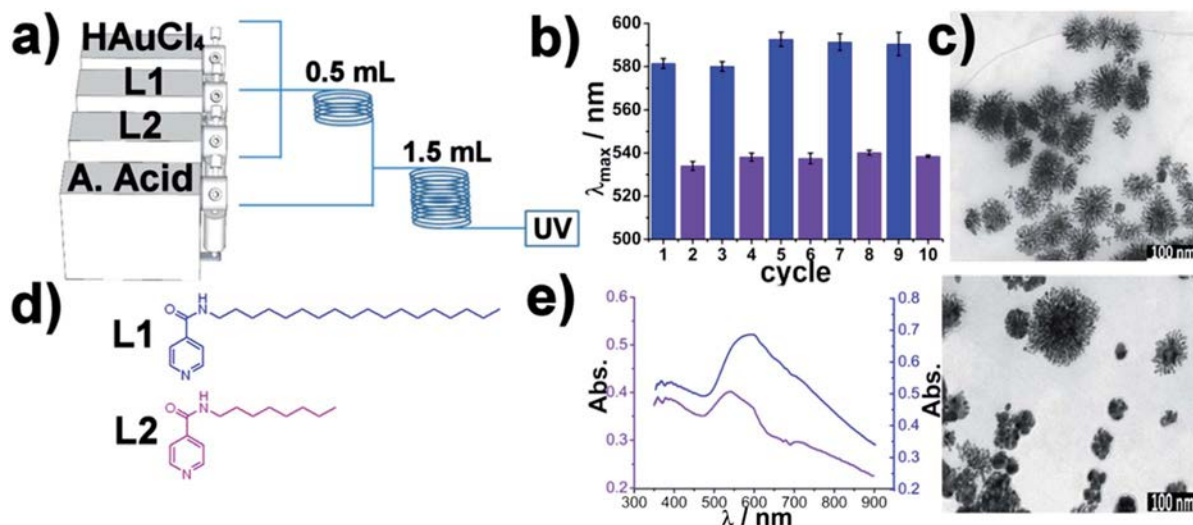
Fig. 3 (a) Reactor scheme. Gold precursor is mixed with the ligands and flown through reactor 1 (R_1) and is subsequently mixed with the reducing agent and flown through reactor 2 (R_2) to an in-line UV-Vis flow cell. After, the samples were collected with an automated fraction collector. Reaction conditions: [Au] = 0.5 mM; [L_1] = [L_2] = 2 mM; [Ascorbic acid] = 5 mM. R.t. t_{R_1} = 0.5 min, t_{R_2} = 1 min. (b) LSPRmax in the different cycles experimented. Odd cycles (blue) were obtained with L_1 and even cycles (violet) correspond to L_2. (c) TEM pictures corresponding to the nanoparticles synthesised. Up corresponds to cycle 1 and down to cycle 2. (d) Ligands employed for the hyper-branched nanostructures. (e) Overlaid example of the UV-Vis spectra corresponding to the hyper-branched nanostructures.

ligand employed, the maximum of absorbance was switching between the first two in a completely reproducible way. These plasmons are different to the traditional shapes reported in the literature[20] and therefore a new morphology was expected. This was confirmed by TEM, which showed hyper-branched Au nanostructured materials (Fig. 3c). A higher degree and extension of branching was found when L_1 was employed as the ligand, compared to the use of L_2.

The crystallinity of the nanomaterials was confirmed by HRTEM, see Fig. 4. This is interesting since, although other materials have been reported showing hyper-branched morphology[21,22] such a large degree of branching has never been seen before with gold and this opens up a range of new possible applications in sensors and catalysis. In a separate control experiment, the nanoparticles were stable for more than a week, even though a slight redshift in the plasmon was observed (see ESI Fig. S12†).
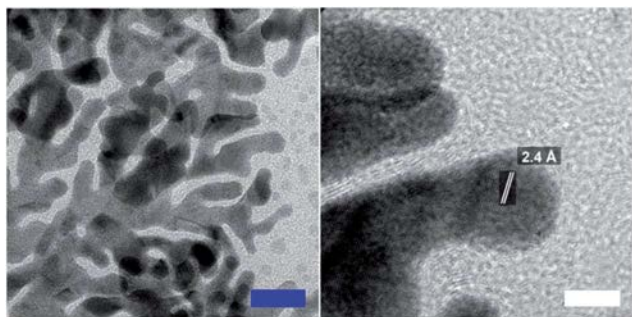

Fig. 4 HRTEM images corresponding to the hyper-branched Au nanostructures synthesized under flow conditions. Blue bar corresponds to a scale of 20 nm. White bar corresponds to a scale of 5 nm.

Conclusions

We have demonstrated the possibility of dynamically controlling the synthesis of AuNPs in continuous-flow assisted by microwave heating and in-line spectroscopic and particle size distribution monitoring. DLS has been employed as an on-line characterisation tool for the synthesis of nanoparticles for the first time, and we show it is possible to control the assembly processes involved in the synthesis of gold nanoparticles. Therefore this approach, with on the fly feedback control, should pave the way to explore the dynamic assembly of a range of other meta-stable or non-equilibrium nanomaterials,[23] especially if other reactor configurations are considered. Moreover, by employing this methodology, we have discovered a new type of hyper-branched gold nanostructures. The exact formation mechanism of these nanostructures remains unclear, but the fractal nature of the nanomaterials might indicate non-equilibrium physical chemical processes such as spinodal decompositions dominating the assembly.[24] In closing we think that this dynamic approach to nanomaterial assembly offers a new route to explore self-assembly, as well as fabricate new material structures and types at the nanoscale with automated control of the experiments and further work will aim at using fitness functions to define the design of new materials *i.e.* discovery as a function of user specification.

Acknowledgements

Notes and references

1 A. Abou-Hassan, O. Sandre and V. Cabuil, *Angew. Chem., Int. Ed.*, 2010, **49**, 6268.

2 J. Wegner, S. Ceylan and A. Kirschning, *Adv. Synth. Catal.*, 2012, **354**, 17.

3 T. N. Glasnov and C. O. Kappe, *Chem.–Eur. J.*, 2011, **17**, 11956.

4 F. Bondioli, A. B. Corradi, A. M. Ferrari and C. Leonelli, *J. Am. Ceram. Soc.*, 2008, **91**, 3746.

5 C. Janzen, H. Wiggers, J. Knipping and P. Roth, *J. Nanosci. Nanotechnol.*, 2001, **1**, 221.

6 J. Wagner and J. M. Köhler, *Nano Lett.*, 2005, **5**, 685.

7 J. Boleininger, A. Kurz, V. Reuss and C. Sonnichsen, *Phys. Chem. Chem. Phys.*, 2006, **8**, 3824.

8 W. Haiss, N. T. K. Thanh, J. Aveyard and D. G. Fernig, *Anal. Chem.*, 2007, **79**, 4215.

9 X. H. Ji, X. N. Song, J. Li, Y. B. Bai, W. S. Yang and X. G. Peng, *J. Am. Chem. Soc.*, 2007, **129**, 13939.

10 V. K. LaMer and R. H. Dinegar, *J. Am. Chem. Soc.*, 1950, **72**, 4847.

11 H. Song, J. D. Tice and R. F. Ismagilov, *Angew. Chem., Int. Ed.*, 2003, **115**, 792.

12 P. J. Kitson, M. H. Rosnes, V. Sans, V. Dragone and L. Cronin, *Lab Chip*, 2012, **12**, 3267.

13 G. Shore, W. J. Yoo, C. J. Li and M. G. Organ, *Chem.–Eur. J.*, 2010, **16**, 126.

14 J. E. Kreutz, L. Li, L. S. Roach, T. Hatakeyama and R. F. Ismagilov, *J. Am. Chem. Soc.*, 2009, **131**, 6042.

15 F. Destremaut, J.-B. Salmon, L. Qi and J.-P. Chapel, *Lab Chip*, 2009, **9**, 3289.

16 J. Turkevich, P. C. Stevenson and J. Hillier, *Discuss. Faraday Soc.*, 1951, **11**, 55; J. Kimling, M. Maier, B. Okenve, V. Kotaidis, H. Ballot and A. Plech, *J. Phys. Chem. B*, 2006, **110**, 15700.

17 W. B. Russel, D. A. Saville and W. R. Schowalter, *Colloidal Dispersions*, Cambridge University Press, 1989.

18 C. J. Richmond, H. N. Miras, A. R. de la Oliva, H. Zang, V. Sans, L. Paramonov, C. Makatsoris, R. Inglis, E. K. Brechin, D.-L. Long and L. Cronin, *Nat. Chem.*, 2012, **4**, 1037.

19 A. R. de la Oliva, V. Sans, H. N. Miras, J. Yan, H. Zang, C. J. Richmond, D.-L. Long and L. Cronin, *Angew. Chem., Int. Ed.*, 2012, **51**, 12759.

20 M. Grzelczak, J. Perez-Juste, P. Mulvaney and L. M. Liz-Marzan, *Chem. Soc. Rev.*, 2008, **37**, 1783.

21 B. Lim and Y. Xia, *Angew. Chem., Int. Ed.*, 2010, **50**, 76.

22 T. K. Sau and C. J. Murphy, *J. Am. Chem. Soc.*, 2004, **126**, 8648.

23 S. C. Warren, O. Guney-Altay and B. A. Grzybowksi, *J. Phys. Chem. Lett.*, 2012, **3**, 2103.

24 S. Fabiano and B. Pignataro, *Chem. Soc. Rev.*, 2012, **41**, 6859.